Atomic Charge-Changing Processes in Plasmas

Viacheslav P. SHEVELKO, Daiji KATO[1)], Hiro TAWARA[1,2)] and Inga Yu. TOLSTIKHINA

P.N. Lebedev Physical Institute, Leninskii prospect 53, Moscow 119991, Russia
[1)]*National Institute for Fusion Science, 322-6 Oroshi-cho, Toki 509-5292, Japan*
[2)]*National Institute of Radiological Science, 4-9-1 Anagawa, Inage-ku, Chiba 263-8555, Japan*

(Received 7 December 2009 / Accepted 19 February 2010)

Properties of various kinds of plasmas are determined by atomic radiation and collision processes occurring between plasma particles, therefore, the detailed knowledge of the effective cross sections and rate coefficients for these processes is highly required. In this work, charge-changing processes, mainly for heavy-particle collisions, including impurity ions, are considered using available computer codes, and the background physics is discussed. Besides general features, the role of *metastable states* of plasma atoms and ions, which are often observed in most of plasmas and play a key role in plasma formation, is considered. The *non-linear* effects observed for heavy particle collisions, such as the *density effect* and *multiple-electron* ionization, are also considered. In addition, the isotope effects are briefly discussed related with electron capture in collisions of alpha particles with hydrogen and its isotopes (D and T).

Keywords: ionization, multiple ionization, electron capture, cross section, metastable state, density effect, hydrogen isotope

DOI: 10.1585/pfr.5.S2012

1. Introduction

Charge-changing processes including electron capture, ionization, three-body recombination, dielectronic recombination, arising in collisions between probe-beam and plasma particles, as well as between plasma particles themselves, play a key role in many aspects of plasma physics (see, e.g., [1–5]). In the present work, the main attention is paid to electron capture,

$$X^{q+} + A \rightarrow X^{(q-1)+} + A^{+}, \tag{1}$$

target ionization

$$X^{q+} + A \rightarrow X^{q+} + A^{+} + e^{-}, \tag{2a}$$

and projectile ionization

$$X^{q+} + A \rightarrow X^{(q+1)+} + \Sigma A + e^{-}, \tag{2b}$$

processes for collisions of X^{q+} ions with neutral atoms A where q denotes an ion charge. To calculate effective cross sections, several atomic codes are used: ARSENY [6], CDW [7] and CAPTURE [8] for electron capture, and ARSENY, DEPOSIT [9], ATOM [1] and LOSS [10] for ionization. A brief description of the codes is given in [11]. The atomic units (a.u.) are used, $m_e = e = \hbar = 1$ where m_e and e denote the electron mass and charge, respectively, and $\hbar$ the Planck constant.

2. General Features

A typical behavior of the charge-changing cross sections as a function of the ion energy E is shown in Fig. 1

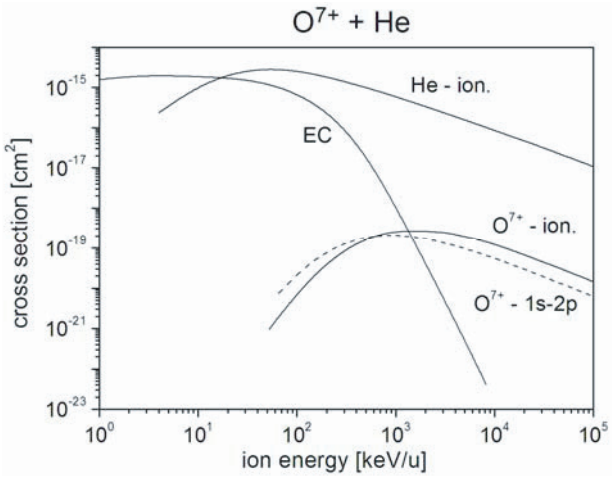

Fig. 1 Calculated ionization and capture cross sections in O^{7+} + He collisions: EC – total electron-capture cross section, He-ion. - ionization of He by O^{7+}, O^{7+}-ion. - ionization of O^{7+} by He, and O^{7+}-1s-2p (dashed curve) - excitation of transition 1s-2p in O^{7+} by He impact.

for O^{7+} + He collisions. Capture and ionization cross sections are denoted as EC and O^{7+}-ion, respectively. As is seen from the figure, electron capture is important at E < 1 MeV/u meanwhile ionization of O^{7+} at E > 1 MeV/u. At ion energies between 500 keV/u and 3 MeV/u, the cross sections of both processes are important. For comparison, cross sections for ionization of He by O^{7+} and excitation cross section (transition 1s-2p) of O^{7+} ions by He atoms are also shown. Different behavior of the electron-capture σ_{ec} and ionization σ_{ion} cross sections as a function of the ion velocity is due to their different dependencies on atomic

author's e-mail: shev@sci.lebedev.ru

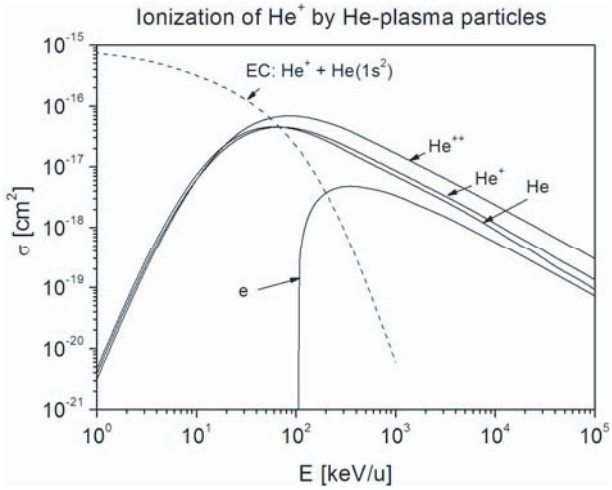

Fig. 2 Calculated ionization sections of He^+ ions by He-plasma particles: electrons (e), He atoms (He) and its ions (He^+, He^{2+}) as a function of He^+ energy; EC denotes electron-capture cross section in $He^+ + He(1s^2)$ collisions. Electron-impact ionization cross section (e) is given in the equivalent energy units showing its threshold behavior.

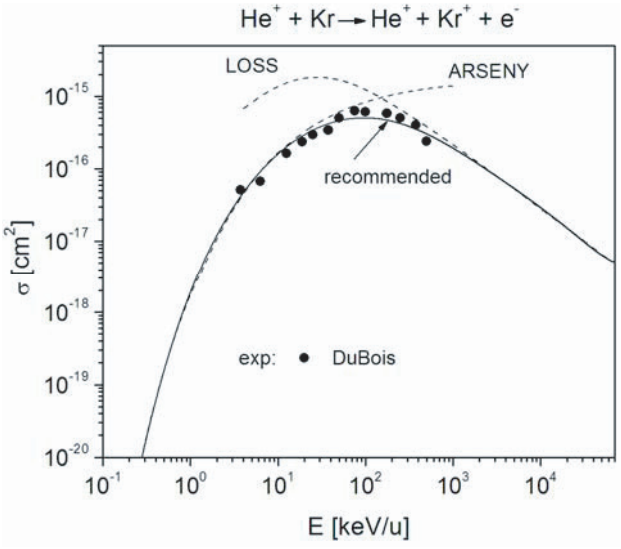

Fig. 3 One-electron ionization cross sections of Kr atoms in collisions with He^+ ions: experiment - solid circles [14], theory - ARSENY code (low energy), LOSS code (high energy), solid curve - recommended cross section, eq. (5).

parameters:

$$\sigma_{ec} \sim \frac{Z^5 q^5}{v^{11} n^3}, \quad N_T \langle v\sigma_{ec} \rangle \sim N_T Z^5 q^5/(v^{10} n^3), \qquad (3)$$

$$\sigma_{ion} \sim \frac{Z^2 n^2}{q^2 v^2} \ln v, \quad N_T \langle v\sigma_{ion} \rangle \sim N_T Z^2 n^2/(vq^2), \qquad (4)$$

where v denotes the relative velocity, Z the effective charge of the target, N_T the target density, n the principal quantum number of the active electron and $<v\sigma>$ the rate coefficient, i.e., the product $v\sigma$ averaged over a Maxwellian velocity distribution of plasma particles. Formulae (3) and (4) are given for relatively high collision velocities.

Interaction cross sections of He^+ ions with He-plasma particles are shown in Fig. 2. The largest ionization cross section of He^+ ions is for collisions with α-particles (He^{2+}) due to the Z^2 dependence ($Z = 2$ in this case). Cross sections for collisions with He and He^+ are nearly of the same size. For comparison, electron-capture (EC) cross section in $He^+ + He(1s^2)$ collisions is also shown in the figure; this symmetric EC is a dominant charge-changing process at energy $E < 50$ keV/u.

Usually various methods of cross-section calculations are applied either at low or high collision energies. In the intermediate energy range, which is often of a high interest, only a few methods exist which can be used for very limited atomic systems like quasi-molecular treatment for one electron in the field of two Coulomb centers (see, e.g., [12]). In such cases, one can apply a well-known formula which uses the known cross-section values at low and high energies and averages them at intermediate energy range:

$$\frac{1}{\sigma_{rec}} = \frac{1}{\sigma_{low}} + \frac{1}{\sigma_{high}}, \qquad (5)$$

where σ_{low} and σ_{high} denote the cross sections calculated at low and high energies, respectively. In Fig. 3, a typical example of such procedure is shown for single-electron ionization of Kr atoms by He^+ ions. At low and high energies two computer codes are applied, ARSENY and LOSS, respectively, which, however, are not valid at intermediate energies $E = 20$ keV/u-300 keV/u. The solid curve represents results of application of eq. (5) which gives quite good agreement with experimental data [13] and can be recommended for the whole energy range considered.

3. Special Features

In this section, some special features of atomic processes involving heavy particles are described such as role of excited (metastable) states of atoms or ions in a plasma or in a probe beam, the density effect, i.e., influence of collision frequency in a high-density plasma, and multi-electron ionization processes. These features can be important for interpretation of experimental results and plasma modeling.

3.1 Role of excited metastable states

The presence of atoms or ions in the excited and, especially, in metastable (long-lived) states in a plasma or a probe beam can change dramatically the interaction cross sections and corresponding rate coefficients. As an example, Figure 4 displays electron-capture cross sections for collisions of $He^+(1s)$ ions with the ground-state $He(1s^2)$ and metastable helium atoms $He^*(1s2s)$. In the latter case, one has to take into account electron capture from two shells, 1s and 2s, meanwhile in collisions with $He(1s^2)$ only 1s-electron is captured. A small bump for $He^*(1s2s)$ target is due to the capture of 2s electron into 2s excited

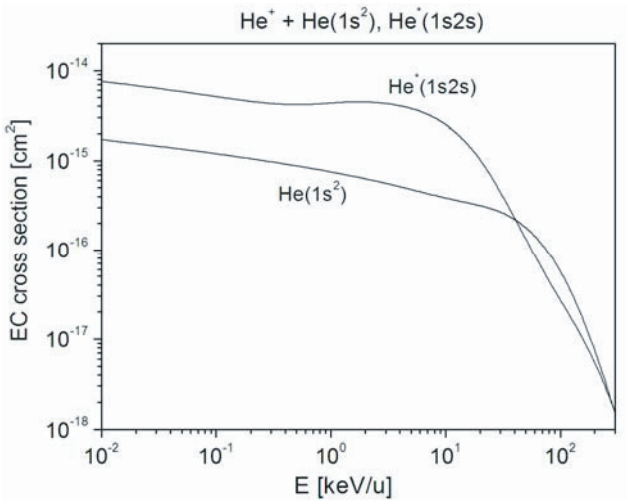

Fig. 4 Calculated electron-capture cross sections in collisions of $He^+(1s)$ ions with He atoms in the ground ($1s^2$) and excited metastable (1s2s) states. In the case of the ground-state He target, the calculated data practically coincide with experimental data [13].

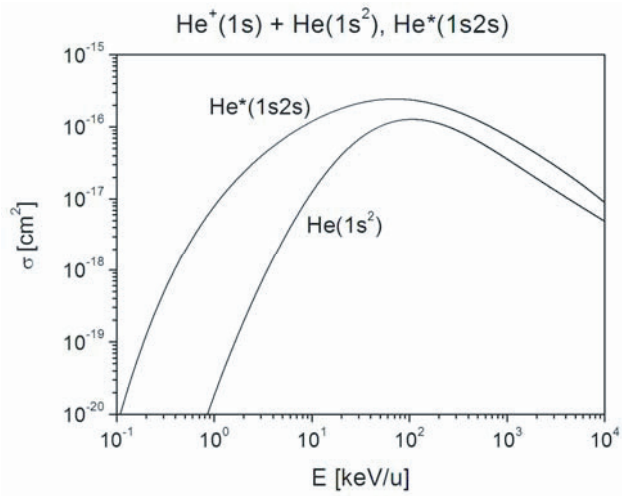

Fig. 5 Calculated ionization cross sections of $He(1s^2, 1s2s)$ atoms in collisions with He^+ ions as a function of He^+ energy. In the case of the ground state He, the calculated data practically coincide with experimental data given in [13].

states. In the case of the ground-state He target, the calculated data practically coincide with experimental data [13]; for $He^*(1s2s)$ target, experimental data are absent. At E < 50 keV/u, electron-capture cross section for $He^*(1s2s)$ target is about 4 times larger than that for $He(1s^2)$ target because of a larger contribution from capture into excited states, (2s-2s) and, therefore, even a small amount of helium atoms in the metastable state can strongly change this charge-changing channel.

Similar comparison of ionization cross sections for the ground-state and excited metastable He atoms by He^+ ions (Fig. 5) also shows an importance of the presence of metastable atoms in a plasma. It is interesting to note that the difference (by 30-40 %) between two ground and metastable state atoms at high energies is due to the contribution of 2s electron which has a low ionization energy resulting in a high ionization efficiency.

3.2 Density effect

In general, the charge-changing cross sections also depend on the plasma density N: with N increasing, the electron capture cross sections σ_{ec} decrease, meanwhile ionization cross sections σ_{ion} increase and, as a result, the mean charge $<q> = \Sigma_i q_i F_i$ of an ion beam after passing through a plasma increases where F_i is the beam equilibrium charge-state fraction with the charge q_i. This effect is called the *target-density* or *gas-solid* effect which depends on the atomic structure of colliding particles, relative collision velocity and the plasma density (see, e.g., [15]). In some cases the effect is very large: it decreases σ_{ec} values up to more than one order of magnitude and increases σ_{ion} values up to a factor of 2.

For electron-capture (1), the cross section is given by a sum over all possible n-states

$$\sigma_{ec} = \sum_{n=n_0}^{n_{cut}} \sigma_{ec}(n), \tag{6}$$

where $\sigma_{ec}(n)$ denotes the partial cross section for the electron capturing into n quantum state to form excited $X^{(q-1)+*}(n)$ ion, n_0 the ground-state number and n_{cut} the maximum quantum number for which $X^{(q-1)+*}(n)$ ions are not ionized through a series of the successive collisions with plasma particles. For low-density plasmas, $n_{cut} \gg 1$, the usual formulae for electron capture and ionization cross sections can be used. However, for high density plasmas, n_{cut} is strongly reduced and can be even closer to the ground-state value n_0.

The excited ion $X^{(q-1)+*}(n)$ can be ionized by the target particles via two channels: by direct ionization or by step-by-step excitation to a certain level also followed by ionization. Correspondingly, two formulae can be applied for estimation of the maximum principal quantum number n_{cut} [15, 16]:

$$n^{d}_{cut} \approx q\left(\frac{10^{18}}{Z^2 N_T[\mathrm{cm}^{-3}]}\right)^{1/7}\left(\frac{v^2}{10q^2}\right)^{1/14} \tag{7}$$

and

$$n^{s}_{cut} \approx q\left(\frac{5\cdot 10^{16}}{Z^2 N_T[\mathrm{cm}^{-3}]}\right)^{1/9}\left(\frac{25v^2}{q^6}\right)^{1/18}. \tag{8}$$

Certainly, $n^s < n^d$, and both n^s and n^d values give the lower and upper limits of the maximum quantum number contributing to electron capture, respectively.

Similar consideration leads to the formula for ionization cross section depending on the plasma density (see [15] in detail).

A typical example of influence of the density effect is shown in Fig. 6 where ionization and capture cross sections are given for 11.5 MeV/u U^{q+} ions passing through

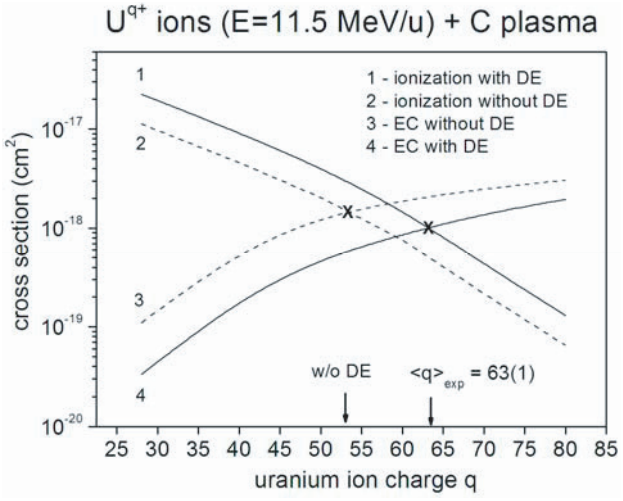

Fig. 6 Ionization and electron-capture cross sections of 11.5 MeV/u U^{q+} ions passing through a carbon plasma with the temperature $T = 3.5$ eV and density $N = 5 \times 10^{19}$ cm^{-3} as a function of uranium ion charge: solid curves - calculated with the density effect (DE), eq. (7), and dashed curves - without DE, $n_{cut} = \infty$. Crosses show the positions of the mean charge of uranium ions: $<q> = 53$ for calculations without DE and $<q> = 62$ with DE accounted for. Experimental value is $<q> = 63 \pm 1$ [17].

a carbon plasma with a temperature of $T = 3.5$ eV and density 5×10^{19} cm^{-3}. Theoretically the mean charge of an ion bean $<q>$ is found from equality between electron capture and loss cross sections at a certain charge q. From Fig. 6 it is seen that the inclusion of the density effect leads to increasing of ionization cross sections by a factor of 2, meanwhile decreasing of capture cross sections by a factor of 4 and, thus, increasing of the mean charge of uranium ions from 53 to 62 units which is in good agreement with experimental value $<q> = 63 \pm 1$ [17]. Generally, when the mean (equilibrium) charge is established, the ionization and electron capture cross sections are expected to be nearly equal as is seen in Fig. 6 with arrows and crosses.

3.3 Multi-electron ionization of heavy ions

If heavy, many-electron ions are involved into plasma atomic collision processes, e.g., as impurity ions or in a probe beam (including heavy negative ions), multi-electron ionization (MI) of both the incident and target particles can be significant even at low-energy regime (see, e.g., experimental works [14], [18]). For example, single-, double- and triple-electron ionization cross sections of U^+ ions colliding with Ar atoms at energy $E = 1.3$ keV/u ($v = 0.23$ a.u.) are 3.2, 1.3 and 0.35×10^{-16} cm^2 [18], respectively, indicating that more than a half of the total cross section originates from MI.

Figure 7 represents calculated total ionization cross sections of W^+ ion, which at present is one of the most interesting subjects for plasma impurity, by electrons, protons, H and He atoms. It is seen that at low energies, ion-

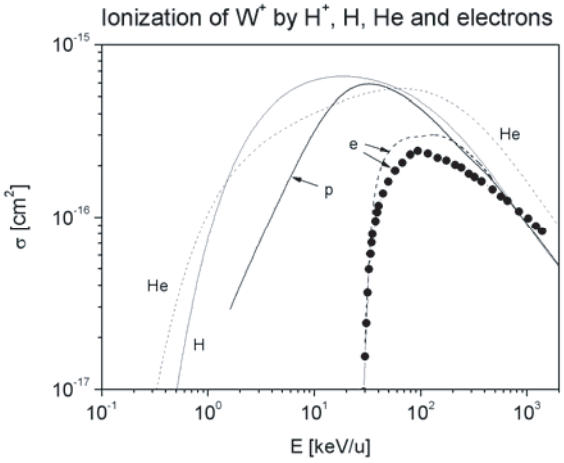

Fig. 7 Calculated total (a sum of single-, double-, triple- etc. ionization cross sections) ionization cross sections of W^+ ions by electrons (e), protons (p), H and He atoms as a function of W^+ energy. Experiment: solid circles - from [19]. Theory: e - electron-impact ionization cross section, ATOM code; p - proton impact, LOSS code, H and He - ionization by H and He atoms, respectively, DEPOSIT and LOSS codes. Electron-impact ionization cross sections are shown as a function of equivalent electron energy for comparison.

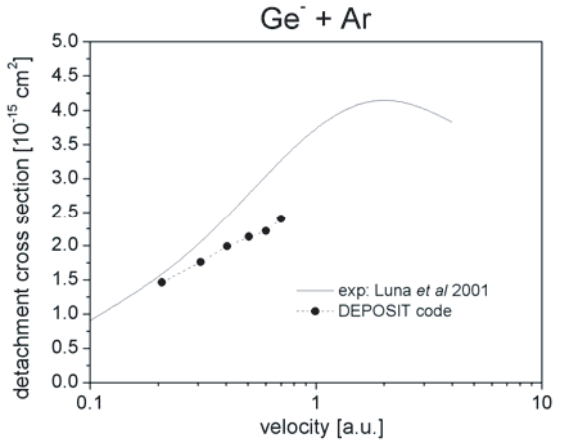

Fig. 8 Calculated electron detachment cross section of negative Ge^- ions by Ar atoms as a function of Ge^- ion energy, DEPOSIT code; solid circles - experiment [20]. Note that 1 a.u. of velocity corresponds to energy of 25 keV/u.

ization by H and He prevails and the corresponding cross sections are extremely large. Influence of electron and proton components is important at rather high energies. At low energies, the main contribution to ionization is due to close collisions and the cross-section value is defined by overlapping volume of electron densities of two colliding particles. At high velocities, ionization cross section depends mainly on the Coulomb field created by target nucleus and electrons.

Another example for ionization of heavy negative ions (detachment cross section) by neutral atoms is shown in Fig. 8 for Ge^- + Ar collisions. The data for MI cross

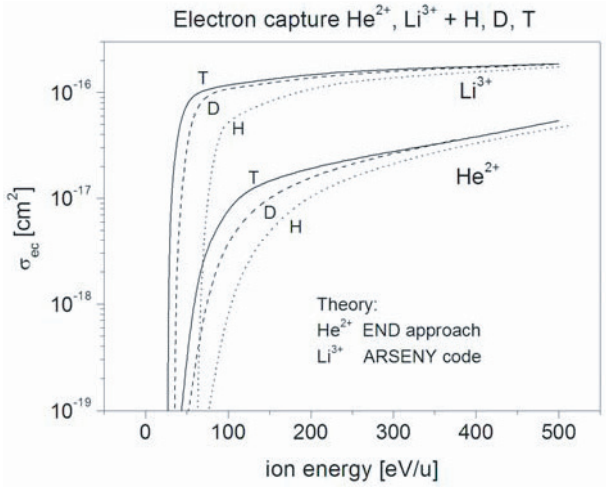

Fig. 9 Calculated electron-capture cross sections for collisions of He^{2+} and Li^{3+} with H, D and T. He^{2+} projectile: the END approach [21]; Li^{3+} projectile: preliminary calculations by ARSENY code, present work (see text).

sections of heavy negative ions, which are also relatively large, are required for analysis and interpretation of the beam-attenuation experiments in plasma probing [23].

4. Isotope Effects

For controlling and modeling the D-T plasma, it is highly desirable to know the cross sections and rates for collisions of alpha particles with D and T atoms. Calculations of the quasi-resonant electron-capture cross sections σ_{ec} for He^{2+} ions colliding with H, D and T targets at ion energies E = 30-1000 eV/u [21] showed that the use of different hydrogen isotopes leads to the large difference in the cross-section values, particularly at low energies. These data were obtained on the basis of the electron-nuclear-dynamics approach (END) by solving the time-dependent Schrödinger equation. The largest difference was found between hydrogen and tritium targets at around 30-50 eV/u where the cross-section ratio is $\sigma_{ec}(T)/\sigma_{ec}(H) \sim 1000$ (Fig. 9). The difference found was explained by isotope effects in the rotational coupling of the quasi-molecule during collision.

In order to compare this influence of isotopic effects for heavier projectile, in the present work the electron-capture cross sections for Li^{3+} + H, D and T were calculated using the ARSENY code (Fig. 9). The code is based on the adiabatic approximation for one-electron transitions in the two-Coulomb-centre system by determining the hidden crossings of the quasi-molecular energy terms. From Fig. 9 it is clearly seen that the isotope effects for Li^{3+} + H, D, T collisions are also very prominent.

5. Rate Coefficients

Rate coefficients, or simply, rates of various atomic processes occurring in laboratory and astrophysical plasmas are of a great importance for many applications in plasma physics (e.g., plasma heating and diagnostics using a probe-beam attenuation), industrial plasmas, astrophysics, astronomy and many others. Usually, a Maxwellian velocity distribution function is applied although other distributions of particles in a plasma can take place [22], e.g., a Maxwellian distribution with two temperatures. This can have a very important consequence for low-temperature plasmas like those in a diverter region.

A special interest is the situation when the ion beam with an arbitrary velocity v_P penetrates a Maxwellian plasma with an arbitrary temperature T. In this case, the rate $<v\sigma>$ of a certain process is defined by the product $v\sigma(v)$ averaged over a new Maxwellian distribution function $F(v, v_P, T)$ depending on v_P and given by

$$\langle v\sigma\rangle = \int_0^\infty v\sigma(v)F(v, v_P, T)\mathrm{d}v \tag{9}$$

with

$$F(v, v_P, T) = \left(\frac{M}{2\pi T}\right)^{1/2} \frac{v}{v_P}\left[\exp\left(-\frac{M}{2T}(v - v_P)^2\right) - \exp\left(-\frac{M}{2T}(v + v_P)^2\right)\right]. \tag{10}$$

Here v denotes the velocity of an incident particle beam relative to plasma particles, and M the reduced mass of colliding particles. This 'new' Maxwellian distribution function $F(v, v_P, T)$ is normalized to unity:

$$\int_0^\infty F(v, v_P, T)\mathrm{d}v = 1. \tag{11}$$

Formula (10) was obtained in [2] and considered further in [23].

At low projectile velocity $v_P \to 0$, the $F(v, v_P, T)$ function, eq. (10), turns into a usual Maxwellian distribution function and at low plasma temperature, $2T/M \to 0$, one has:

$$F(v, v_P, T) = \delta(v - v_P), \tag{12}$$

and

$$\langle v\sigma(v)\rangle \approx v\sigma(v). \tag{13}$$

Equation (13) is commonly used in plasma physics for estimating rate coefficients when the projectile velocity is much higher than the thermal plasma velocity v_T, i.e., $v_P \gg v_T$ (see, e.g., [24]) where the thermal velocity v_T corresponds to the maximum of a Maxwellian distribution function:

$$v_T \approx 1.13\sqrt{2T/M}. \tag{14}$$

In eq. (13), v is the relative velocity given as

$$v \approx \sqrt{v_P^2 + v_T^2}. \tag{15}$$

If the projectile velocity is smaller than the thermal velocity, $v_P \le v_T$, the exact general formulae (9) and (10)

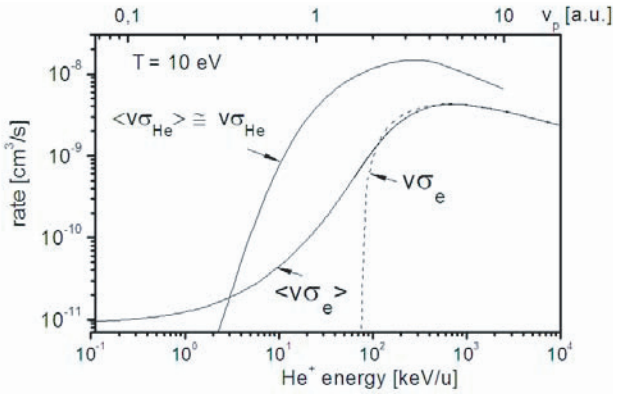

Fig. 10 Calculated rate coefficients for electron-impact (labeled by e) and He-impact ionization of He^+ ions passing through He plasma with a temperature $T = 10$ eV as a function of He^+ energy: solid curves - exact formulae for $<v\sigma>$, eqs. (9)-(10); dashed curve - approximate formula, $v\sigma$, eq. (13). The corresponding helium-ion velocity v_P is displayed in the upper scale. In the case of He impact, the rates obtained with the exact and approximate formulae practically coincide.

should be used.

Figure 10 shows the rates for ionization of He^+ ions by He atoms (labeled by He) and electrons (e) when He^+ ions with velocity v_P penetrate He plasma with a temperature $T = 10$ eV. In the case of He target, the thermal velocity v_T(He) ≈ 0.01 a.u., $v_P \gg v_T$ in the whole range of v_P and ionization rates calculated by eqs. (9) or (13) give practically the same results, $<v\sigma_{He}> \approx v\sigma_{He}$.

In the case of ionization by electron impact, the situation is different because the electron-impact ionization cross section σ_e of He^+ has a sharp threshold on electron energy at $E_{th} = I(He^+) \approx 54.4$ eV corresponding to threshold velocity $v_{th} \approx 2$ a.u. From eq. (13) it follows that at projectile velocities $v_P < 2$ a.u. one has $\sigma_e = 0$ and, therefore, the rate given by the product $v\sigma_e = 0$. But due to the exponential tail of the distribution function (10), the averaged rate $<v\sigma_e>$ is not zero even for $v_P < 2$ a.u. This difference is seen in Fig. 10 by comparing two curves for ionization rates induced by electron impact: for projectile velocities $v_P < 2$ a.u. there is a big difference between rates given by approximate, eq. (13) and by exact, eqs. (9) and (10) formulae. In general, eqs. (9) and (10) give the exact expression of the rate coefficients for an arbitrary projectile velocity and plasma temperatures.

6. Conclusion

Charge-changing atomic processes in plasmas are considered in terms of effective cross sections and rate coefficients with a Maxwellian velocity distribution function. Some general features have been demonstrated for the cross sections (dependencies on velocity, ion charge and target charge) as well as specific properties (role of metastable states, multi-electron ionization, density effect) which are illustrated by computer calculations performed using available computer codes. It is also pointed out that the isotope effects are expected to be large in electron-capture cross sections among hydrogen isotope targets (H, D and T) at very low collision energies $E < 200$ eV/u.

Special attention is paid to the case when an ion beam penetrates a plasma with a certain temperature and it was shown that one has to use the exact general formula for the rate $<v\sigma>$ averaged with a 'new' Maxwellian function depending on the beam velocity v_P. In calculating the effective cross sections at low collision energies, one has to take into account the isotope effects, i.e., dependence on the reduced mass of colliding particles.

Acknowledgments

This work is partially supported by the NIFS/NINS project of Foundation Network for Scientific Collaboration.

[1] L.A. Vainshtein and V.P. Shevelko, *Atomic Physics for Hot plasmas* (IOP, Bristol, 1985).
[2] R.K. Janev, W.D. Langer, K. Evans and Jr., D.E. Post, *Elementary Processes in Hydrogen-Helium Plasmas: Cross Sections and Reaction Rate Coefficients* (Springer, Berlin, 1987).
[3] Y. Itikawa, *Molecular Processes in Plasmas: Collisions of Charged Particles with Molecules* (Springer, Berlin, 2007).
[4] I.Yu. Tolstikhina, P.R. Goncharov, T. Ozaki *et al.*, *Electric Charge State Changing Collisions of Hydrogen and Helium with Low-Z Impurity Particles*, Report NIFS-DATA-102 (NIFS, Toki, Japan, 2008).
[5] H.-J. Kunze, *Introduction to Plasma Spectroscopy* (Springer, Berlin, October 2009).
[6] E.A. Solov'ev, Sov. Phys. - Uspekhi **32**, 228 (1989).
[7] Dž. Belkic, R. Gayet and A. Salin, Comput. Phys. Commun. **23**, 153 (1981); *ibid.* **32**, 385 (1984).
[8] V.P. Shevelko, O. Rosmej, H. Tawara and I.Yu. Tolstikhina, J. Phys. B **37**, 201 (2004).
[9] V.P. Shevelko, M.S. Litsarev and H. Tawara, J. Phys. B **41**, 115304 (2008) ; V.P. Shevelko, D. Kato, M.S. Litsarev and H. Tawara, J. Phys. B **43**, 215202 (2010).
[10] V.P. Shevelko, I.Yu. Toltikhina and Th. Stöhlker, Nucl. Instrum. Meth. B **184**, 295 (2001).
[11] V.P. Shevelko, D. Kato, M.-Y. Song *et al.*, Nucl. Instrum. Meth. B **267**, 3395 (2009).
[12] E.A. Solov'ev, Sov. Phys. - Uspekhi **32**, 228 (1989).
[13] R. Ito, T. Tabata, T. Shirai and R.A. Phaneuf, Report JAERI-M-117 (Japan, 1993).
[14] R.D. DuBois, Phys. Rev. A **39**, 4440 (1989).
[15] V.P. Shevelko, H. Tawara, O.V. Ivanov *et al.*, J. Phys. B **38**, 2675 (2005).
[16] I.Yu. Tolstikhina and V.P. Shevelko, 22nd SPIG, AIP Conf. Proc. Vol. **740** (2004) pp.59-66.
[17] H. Wahl, M. Giessel, A.A. Golubev *et al.*, Short. Commun. Phys. **8**, 28 (Lebedev Institute, Moscow 2001).
[18] H.H. Lo and W.L. Fite, At. Data **1**, 305 (1970).
[19] H. Tawara and M. Kato, NIFS-DATA-51 (NIFS, Japan, 1999).
[20] H. Luna, F. Zappa, M.H.P. Martines *et al.*, Phys. Rev. A **63**, 052716 (2001).
[21] N. Stolterfoht, R. Cabrera-Trujillo, Y. Ohrn *et al.*, Phys.

Rev. Lett. **99**, 103201 (2007).
[22] M. Lamoureux, Adv. At. Mol. Phys. **31**, 223 (1993).
[23] M. Nishiura, H. Tawara, T. Ido *et al.*, Report NIFS-884 (Toki, Japan, Jan. 2008).
[24] Th. Peter and J. Meyer-ter-Vehn, Phys. Rev. A **43**, 2015 (1991).